

COLLINEAR CLUSTER TRIPARTITION: FIRST STEPS IN PHYSICAL TREATING

D.V. KAMANIN, A.A. ALEXANDROV, I.A. ALEXANDROVA,
N.A. KONDTATYEV, E.A. KUZNETSOVA, O.V. STREKALOVSKY,
V.E. ZHUCHKO

Joint Institute for Nuclear Research, 141980 Dubna, Russia;

YU.V. PYATKOV

*Joint Institute for Nuclear Research, 141980 Dubna, Russia, Moscow Engineering
Physics Institute, 115 409 Moscow, Russia;*

W. von OERTZEN

Helmholz-Zentrum Berlin, 14109 Berlin, Germany

Preliminary results of the analysis of the rectangular structures in the mass correlation distributions of the fission fragments from ^{252}Cf (sf) are presented. The structures lie in the region of big missing mass and are connected with the multi-body decay of the mother system. The ternary chain-like pre-scission configuration seems to be too compact and could decay due to tunneling only. More elongated four-body configuration leading to the quaternary decay let meet energy conservation law in the scission point.

1. Introduction

In our recent publications [1–3] we have summarized experimental evidences of existing of a new type of ternary decay of heavy low excited nuclei called by us collinear cluster tri-partition (CCT). The results obtained inspired the series of theoretical works dedicated to the CCT process [4–7]. Theoretical predictions put forward are based on the comparison of the energy prices of different pre-scission nuclear configurations leading to the ternary decay. Possible kinetic energies of all decay partners are estimated as well in ref. [3].

Bearing in mind all the predictions to be strongly model dependent we have compared them with our experimental results for choosing the most realistic ones. We discuss as well our own scenarios of some of the CCT modes.

2. Experimental data

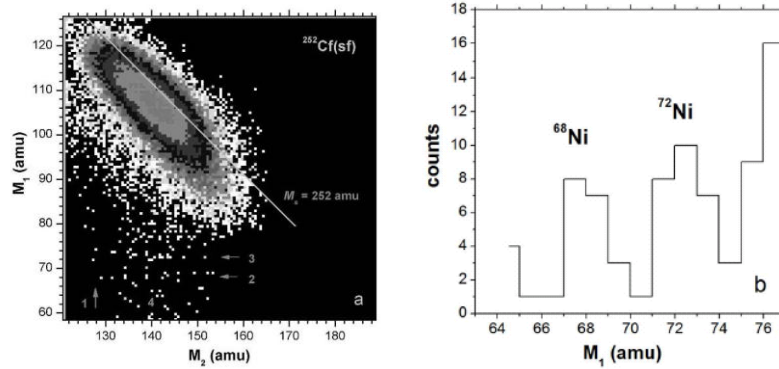


Figure 1. The region of the mass-mass distribution for the FFs from $^{252}\text{Cf}(sf)$ around the CCT bump. No additional gates were applied (there is no background of scattered fragments) due to the use of PIN diodes as “stop” detectors. An internal structure of the “bump” consisting of the lines $M_{1,2} = \text{const}$ (marked by the numbers 1–3) and tilted lines $M_1 + M_2 = \text{const}$ (number 4) are seen. The lines marked by the arrows, 2 and 3 are shown in Figure 1b as a projection.

Two tilted diagonal lines with $M_s = M_1 + M_2 = 196$ amu and $M_s = 202$ amu (marked by number 4) which start from the partitions 68/128 and 68/134, respectively, are also seen.

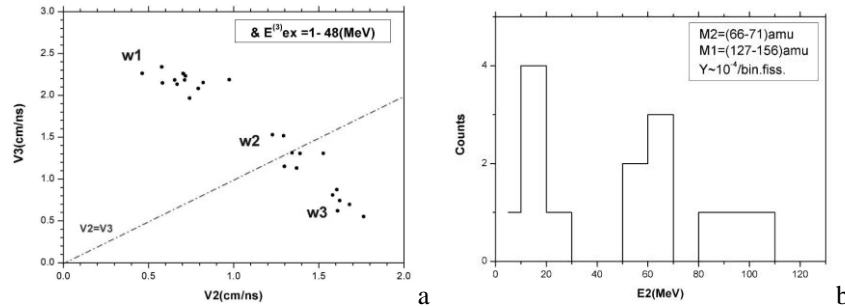


Figure 2. Velocities of the fragments from ternary decay having lightest (V_3) and middle (V_2) masses – a. Energy spectrum of the Ni fragments from the events marked by number 2 in Figures 1a – b.

Actually only two fragments were detected in each decay event. Mass and velocity of the “missed” fragment were calculated basing on the mass and momentum conservation laws. Figure 2a demonstrates a correlation between the velocities of two lighter partners of the ternary decay. For the sake of convenience, the FFs from ternary events are labeled by numbers 1–3 in an order of decreasing their masses. Three different groups of events are vividly seen in the figure. They are marked by the signs w1–w3 respectively. We will

analyze the events of each group separately. Energy spectrum of the detected Ni ions is shown in Figure 2*b*. Their yield does not exceed 10^{-4} per binary fission.

3. Possible physical scenarios for the events based on Ni clusters

The basic properties of the events joined in *w1*-group are presented in Figure 3*a*. Possible scenarios of the decay standing behind are illustrated by Figures 3*b*, *c*.

Comparing the velocities of the decay partners for typical event from *w1*-group one can suppose that the precission configuration looks like as shown in Figure 3*a*. Really, $V_1 \sim V_{H_bin}$ where V_{H_bin} typical velocity of the heavy fragment in conventional binary fission. It means that the first rupture took place between ^{142}Cs and di-nuclear system $^{42}\text{P}/^{68}\text{Ni}$. The charges of the FFs were calculated in the frame of the unchanged charge density hypothesis (“ Z_{ucd} hypothesis”), except of ^{68}Ni which nucleon composition is due to the neutron subshell $N = 40$ [8]. The second rupture likely appeared to occur after full acceleration of the di-nuclear system $^{42}\text{P}/^{68}\text{Ni}$ because $V_3 > V_2$. At the same time the precission configuration proposed contradicts to the energy conservation law. Interaction energy E_{int} between the nuclei in the chain (taking into account both Coulomb and nuclear components) which converts to the total kinetic energy after scissions exceeds Q_3 -value. It means that the decay according to the scenario proposed could take place due to the tunneling only. Of course, deformation (elongation) of the decay partners could decrease Coulomb energy but some part of the free energy must be paid as the deformation energy in this case. The following alternative scenario seems to be more realistic (Figure 3*b*).

As can be inferred from Figure 1*a* the rectangular structures are due both to the heavy and light magic clusters and they manifest themselves by the same way. One observes both the line $M_1 = \text{const}$ and $M_2 = \text{const}$. It is reasonable to suppose that both magic clusters are preformed at least at the scission configuration. It means that it can look like as a chain of nuclei shown in Figure 3*b*. But it appears $Q_4 > E_{int}$ as it was in the previous case. Supposing that the partners 3 and 4 (Figure 3*b*) move after first rupture as a single di-nuclear system we can decrease energy deficit, but still $E_{int}(1, 2_3 + 4) > Q_4$. At last changing nucleon composition of two lighter nuclei in order to maximize Q_4 value one succeeds to meet energy conservation law (Figure 3*c*).

Similar consideration was performed for the events from *w2*-group (Figure 4). The closeness of the velocities $V_3 \sim V_2$ can be explained by the specific mechanism of the “dynamical blocking”. We mean the following scenario. The first rupture appeared to occur between the heavy nucleus of ^{143}Cs and di-

nuclear system of $^{70}\text{Ni}/^{39}\text{P}$. Immediately after this the second rupture making ^{142}Cs nucleus free took place (Figure 4a). Nucleus of ^{39}P being lighter than the ^{70}Ni nucleus will run down it very soon but cannot outrun because the path is blocked (“dynamical blocking”). Cinematically for the Cs nucleus both nuclei move as a single system. Strong support for such scenario follows from the fact that $M_{1exp} \sim M_{1TT}$, where M_{1exp} – is the actually measured mass of heavy fragment (using “ $V-E$ ” method) while M_{1TT} – the mass calculated for binary fission approach (i.e. in the frame of the “TOF–TOF” method). The scenario proposed explains the velocity correlations observed but contradicts to the energy conservation law ($E_{int} > Q_3$), i.e. cold fission via compact ternary configuration is interdicted (except of tunneling provided low probability of the decay).

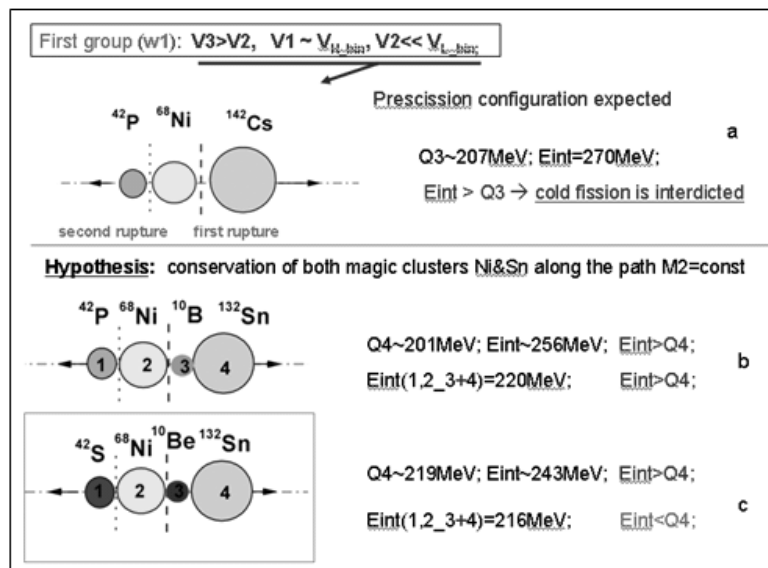


Figure 3. Parameters of the events from w1-group – a, possible precision configuration for these events under condition that nucleon composition of the light partners follow Z_{ucd} hypothesis – b, similar configuration for the best Q_4 -value – c.

Basing on the same arguments as in the previous case we suppose an elongated precision configuration from four nuclei (Figure 4b). Relatively long distance between Ni and Sn nuclei decreases total Coulomb energy and E_{int} estimated for the sequence of ruptures shown in Figure 4b becomes less

than Q_4 even without its maximizing by variation of the nucleon composition of lighter decay partners. Thus quaternary decay is expected.

The events from the $w3$ -group were analyzed in the same manner as those from two previous groups. Corresponding illustrations are presented in Figure 5. Once more $V_1 \sim V_{H_bin}$ is observed while $V_3 < V_2$. In order to reproduce the experimental velocity correlations the first rupture is supposed to occur between heavy Cs nucleus and di-nuclear system of Ni/P. After full acceleration this system decays making free both constituents. The compact ternary configuration provides too high expected total kinetic energy exciding Q_3 -value (Figure 5a).

Decay via elongated configuration shown in Figure 5b overcomes this difficult. The sequence of ruptures different from the scenario for $w2$ -group changes the velocity of ^{39}P nucleus (the di-nuclear system Ni/P decays on-the-fly). Also quaternary decay channel is predicted in the frame of the proposed scenario.

Thus almost similar nuclear composition, but different sequence of partners and rupture scenarios are actually realized giving rise to the different kinematics of the partners involved.

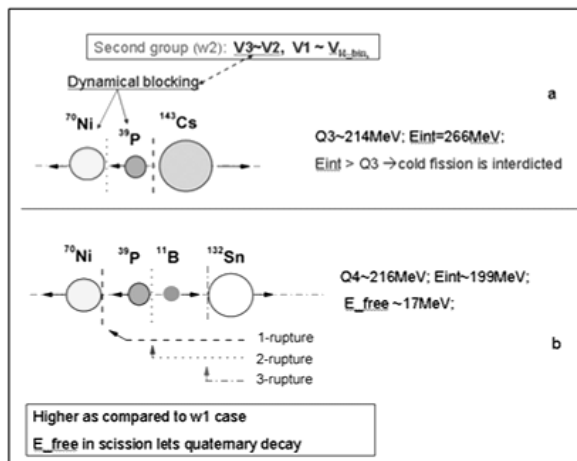


Figure 4. Parameters of the events from $w2$ -group – *a*, possible precission configuration for these events – *b*.

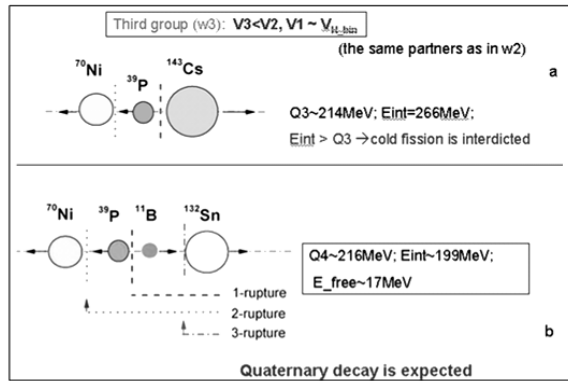


Figure 5. Parameters of the events from w3-group – a, possible precission configuration for these events – b.

4. Possible physical scenarios for the events forming tilted ridges

We come to the analysis of the structures which look like the tilted ridges in Figure 1a. Along each ridge the following expression is valid $M_1 + M_2 = \text{const}$ what means that $M_3 = \text{const}$ for the missed fragment. Expected decay scenario for the events is illustrated by Figure 6.

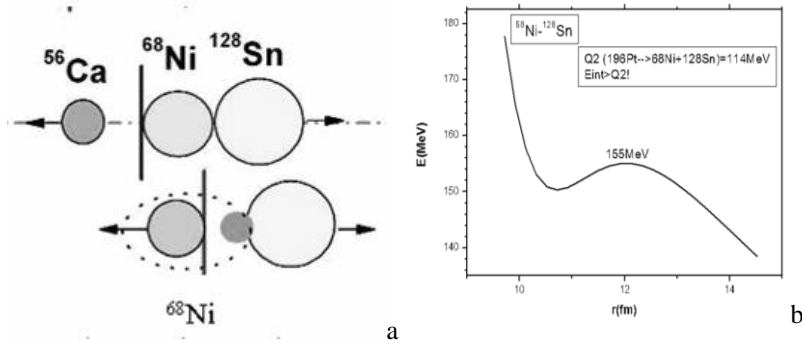


Figure 6. Two-stage decay process giving rise presumably to one of the tilted ridges in fig. 1a – a; interaction potential between the fragments at the second stage of the decay – b.

The most left tilted ridge in the figure starts from the partition $^{68}\text{Ni}/^{128}\text{Sn}$. It means that ^{56}Ca nucleus is missed in this point (the upper scheme in Figure 6a) and along all the ridge as well. If one moves along the ridge the mass of the light fragment detected decreases while heavy fragment becomes more and more heavy “nipping off” the nucleons from the Ni cluster. Figure 6b gives an idea why it happens. Potential energy of the di-nuclear system $^{68}\text{Ni}/^{128}\text{Sn}$ is higher than Q -value for the decay $^{196}\text{Pt} \rightarrow ^{68}\text{Ni} + ^{128}\text{Sn}$. The decay of Pt nucleus can appear to occur from more elongated shape only. Elongation of the

^{68}Ni cluster to be softer than magic nucleus of ^{128}Sn likely realizes via its clusterization. The process is very close to this predicted by the Ikeda rule [9] for the light nuclei.

5. Comparison of the results with model calculations

For the moment at least two theoretical works are known to be dedicated to kinematical parameters of the decay partners of the collinear ternary decay [5, 6]. Only one CCT combination namely Sn-Ca-Ni is analyzed in the frame of a simplified model in ref. [5]. Nevertheless, a principal peculiarity of the energy spectra of the light CCT partners is reproduced, namely their two-component composition (low energy and high energy peaks). Our data from $w1$ and $w2$ groups are shown in Figure 7. Energies were estimated for the three body precession configurations basing on the total E_{int} and momentum conservation in two-step sequential process. The upper high energy group of the events corresponds to the precession configuration shown in Figure 3a. Similar calculations for the configuration from Figure 4a give low energy group in Figure 7. Our results agree with the predictions of work [5] even quantitatively. But as we showed above such decays could appear to occur due to tunneling only. Rather close approach was used in ref. [6].

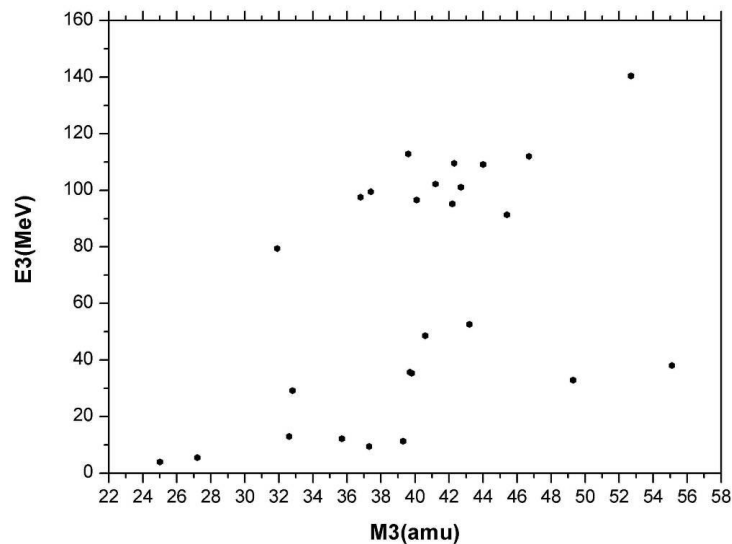


Figure 7. Masses and energies of the lightest CCT partner. Energies were estimated for the three body precession configuration. See text for details.

6. Conclusions

1. Strict energy restrictions rule the CCT process what results in variety of exit kinematical parameters of the CCT partners in dependence of their precission configuration and time scenario of the ruptures.
2. More consistent theoretical models are needed for realistic description of the CCT process.

References

1. Yu. Pyatkov et al., *Eur. Phys. J.* **A45**, 29 (2010).
2. Yu. Pyatkov et al., *Bulletin of the Russian Academy of Sciences. Physics.* **75**, 949 (2011).
3. Yu. Pyatkov et al., *Eur. Phys. J.* **A48**, 94 (2012).
4. K. Vijayaraghavan et al., *Eur. Phys. J.* **A48**, 27 (2012).
5. R. Tashkhodjaev et al., *Eur. Phys. J.* **A47**, 136 (2011).
6. K. Manimaran et al., *Eur. Phys. J.* **A45**, 293 (2010).
7. V. Pashkevich et al., *Int. Journal of Modern Phys.* **E19**, 718 (2010).
8. D. Rochman et al., *Nucl. Phys.* **A735**, 3 (2004).
9. H. Horiuchi, K. Ikeda, *Cluster Model of the Nucleus*. Int. Rev of Nucl. Phys. Eds. T. T. S. Kuo and E. Osnes. V. 4. (World Scientific, Singapore, P. 1. (1986).